Magnetoelectric resonances and predicted microwave diode effect of the skyrmion crystal in a multiferroic chiral-lattice magnet

Masahito Mochizuki[1,2,*] and Shinichiro Seki[3]

[1]*Department of Applied Physics, The University of Tokyo, Tokyo 113-8656, Japan*

[2]*Institute of Theoretical Physics, University of Cologne, D-50937 Cologne, Germany*

[3]*Department of Applied Physics and Quantum Phase Electronics Center, The University of Tokyo, Tokyo 113-8656, Japan*

(Received 20 September 2012; published 3 April 2013)

We theoretically discover that unique eigenmodes of skyrmion crystal (SkX) are not only magnetically active to an ac magnetic field ($\boldsymbol{H}^{\omega}$) but also electrically active to an ac electric field ($\boldsymbol{E}^{\omega}$) in a multiferroic chiral-lattice magnet Cu_2OSeO_3, which amplifies the dynamical magnetoelectric coupling between $\boldsymbol{E}^{\omega}$ and the spin texture. The resulting intense interference between their electric and their magnetic activation processes can lead to an unprecedentedly large diode effect on the microwave, i.e., its absorption by SkX changes up to ∼20% when the incident direction is reversed. Our results demonstrate that the skyrmion could be a promising building block for microwave devices.

DOI: 10.1103/PhysRevB.87.134403 PACS number(s): 76.50.+g, 75.10.Hk, 75.70.Ak, 75.78.−n

Skyrmion, a topological vortex-like swirling spin texture,[1] is now attracting a great deal of interest. It was predicted that the skyrmion and its crystallized form, so-called skyrmion crystal (SkX), are realized in chiral-lattice magnets without inversion symmetry through competition between ferromagnetic (FM) and Dzyaloshinskii-Moriya (DM) interactions under a magnetic field $\boldsymbol{H}$.[2,3] Quite recently, the SkX phase was indeed observed in metallic B20 alloys such as MnSi,[4–7] $Fe_{1-x}Co_xSi$,[8,9] and FeGe,[10] as well as in the insulating magnet Cu_2OSeO_3,[11–13] by small-angle neutron-scattering (SANS) experiments and Lorentz transmission electron microscopy (LTEM).

Since then, several experiments have been performed and have reported intriguing transport properties in SkX[14–19] and electric control of skyrmions with spin-polarized current[20,21] in *metallic* systems. The emergence of spin-driven ferroelectric polarization $\boldsymbol{P}$ has been observed in the *insulating* SkX phase of Cu_2OSeO_3,[11,22,23] and the electric-field control of this *multiferroic* skyrmion texture was experimentally demonstrated.[24] There the research interest, more or less, comes from the possible application to next-generation spintronics devices. However, a lot of researchers are presaging further potentiality in skyrmions. Nevertheless, the sorts of experimental work are quite limited, i.e., observations by means of LTEM or SANS and transport measurements only.

In this article, we theoretically propose a brand new direction for the research on skyrmions from the viewpoints of microwave functionalities and dynamical phenomena at gigahertz frequencies. We discover that collective rotational and breathing motions of skyrmions in SkX can be resonantly activated not only by an ac magnetic field ($\boldsymbol{H}^{\omega}$) but also by ac electric field ($\boldsymbol{E}^{\omega}$) as unique eigenmodes of SkX in multiferroic chiral-lattice magnets. These resonances amplify the dynamical coupling of underlying spin texture with $\boldsymbol{E}^{\omega}$ and $\boldsymbol{H}^{\omega}$, and the resulting intense interference between the electric and the magnetic activation processes can lead to unprecedentedly large directional dichroism of the electromagnetic (EM) wave in Cu_2OSeO_3; i.e., its absorption by SkX changes up to ∼20%, depending on the sign of its incident direction. This effect is enhanced especially at eigenfrequencies of the aforementioned skyrmion resonances (∼GHz) and can work as an efficient microwave diode. Currently, most microwave-device functions are achieved using designed combinations of waveguides, circuits, and elements made of ferrites with ferrimagnetic order.[25] Our finding provides a guideline for designing new microwave devices such as a magnetically tunable isolator. Our work will be a trigger for a broad-based quest for novel functions of skyrmions and related spin textures.

The magnetic structure of Cu_2OSeO_3 is composed of tetrahedra of four Cu^{2+} ($S = 1/2$) ions as shown in Fig. 1(a). Recent powder neutron diffraction[26] and NMR[27] experiments suggested that a three-up- and one-down (*uuud*)-type collinear spin arrangement is realized on each tetrahedron below $T_c \sim 58$ K. We regard this four-spin assembly as a magnetic unit and treat it as a classical vector spin $\boldsymbol{m}_i$ whose norm m is unity. We employ a classical Heisenberg model on a cubic lattice[28–30] to describe the magnetism in a thin specimen of Cu_2OSeO_3, which contains the FM-exchange interaction, the DM interaction,[31] and the Zeeman coupling to the external $\boldsymbol{H}$ normal to the plane. The Hamiltonian is given by

$$\mathcal{H}_0 = -J\sum_{\langle i,j\rangle}\boldsymbol{m}_i\cdot\boldsymbol{m}_j - D\sum_{i,\hat{\boldsymbol{\gamma}}}\boldsymbol{m}_i\times\boldsymbol{m}_{i+\hat{\boldsymbol{\gamma}}}\cdot\hat{\boldsymbol{\gamma}} - g\mu_B\mu_0 H_z\sum_i m_{iz}, \quad (1)$$

where $g = 2$, and $\hat{\boldsymbol{\gamma}}$ runs over $\hat{\boldsymbol{x}}$ and $\hat{\boldsymbol{y}}$. We set the ratio $D/J = 0.09$, for which the periodicity in the SkX phase becomes ∼99 sites. Since the distance between adjacent Cu-ion tetrahedra is ∼5 Å, this periodicity corresponds to a skyrmion diameter of ∼50 nm, in agreement with the LTEM observation.[11] All the spin textures considered here are slowly varying, which can be described by a continuum spin model. It justifies our treatment based on a lattice spin model after division of the space into square meshes and coarse graining of magnetizations.

We first analyze the model, (1), using the replica-exchange Monte Carlo technique and obtain the phase diagrams at low temperature (T) shown in Fig. 1(b). The SkX phase emerges

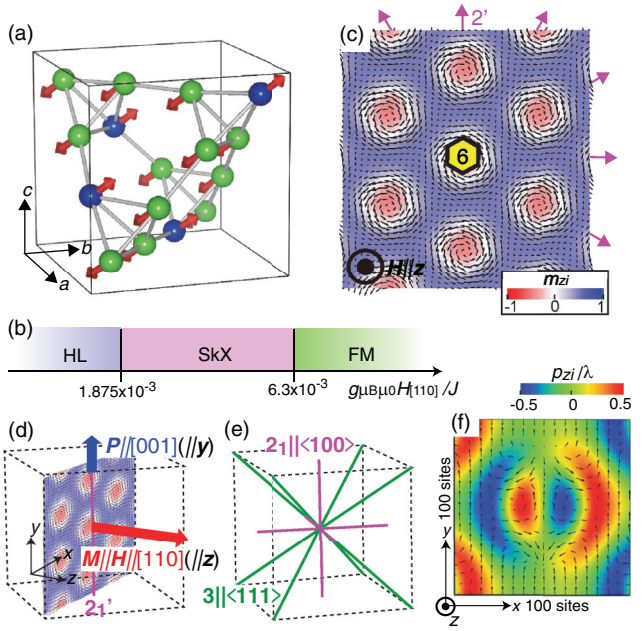

FIG. 1. (Color) (a) Spin structure of Cu_2OSeO_3, composed of tetrahedra of four Cu^{2+} ions ($S = 1/2$) with three-up and one-down spins. (b) Phase diagram of the spin model, (1). Here HL, SkX, and FM denote the helical, skyrmion-crystal, and ferromagnetic phases, respectively. (c) Spin structure in the SkX phase, which possesses a sixfold rotation axis, 6, and six twofold rotation axes, followed by time reversal, $2'$. Arrows represent in-plane spin components. (d) Under $\boldsymbol{H} \parallel [110]$, the system becomes polar along [001] and the emergence of ferroelectric polarization $\boldsymbol{P} \parallel [001]$ is allowed. (e) Symmetry axes in a Cu_2OSeO_3 crystal, which belongs to the $P2_13$ space group: threefold rotation axes, 3, along $\langle 111 \rangle$ and twofold screw axes, 2_1, along $\langle 100 \rangle$. (f) Real-space configurations of local electric polarizations $\boldsymbol{p}_i$ in the skyrmion under $\boldsymbol{H} \parallel [110]$.

in the range $1.875 \times 10^{-3} < |g\mu_B\mu_0 H_z/J| < 6.3 \times 10^{-3}$, sandwiched by the helical and FM phases, in agreement with the experiment for thin-plate samples.[11] Skyrmions are crystallized into a triangular lattice and magnetic moments $\boldsymbol{m}_i$ directly antiparallel (parallel) to $\boldsymbol{H}$ at the center (periphery) of each skyrmion as shown in Fig. 1(c).

For the SkX state formed under $\boldsymbol{H} \parallel [110]$ as shown in Fig. 1(d), the emergence of $\boldsymbol{P} \parallel [001]$ perpendicular to the net magnetization $\boldsymbol{M} \parallel \boldsymbol{H}$ is expected from symmetry considerations. As shown in Fig. 1(e), the crystal structure of Cu_2OSeO_3, which belongs to a nonpolar space group, $P2_13$, possesses threefold rotation axes, 3, along $\langle 111 \rangle$ and 2_1-screw axes along $\langle 100 \rangle$. The spin texture in the SkX phase is also nonpolar, with a sixfold rotation axis, 6, along $\boldsymbol{H}$ and twofold rotation axes followed by time reversal, $2'$, normal to $\boldsymbol{H}$ as shown in Fig. 1(c). When the SkX sets in under $\boldsymbol{H} \parallel [110]$ on the Cu_2OSeO_3 crystal, most of the symmetries should be broken, and only the $2_1'$ axis ($\parallel [001]$) normal to $\boldsymbol{H}$ survives, as shown in Fig. 1(d). Consequently, the system becomes polar along [001]. Indeed the emergence of $\boldsymbol{P} \parallel [001]$ under $\boldsymbol{H} \parallel [110]$ was experimentally observed.[23] Here we define the Cartesian coordinates, $\boldsymbol{x} \parallel [\bar{1}10]$, $\boldsymbol{y} \parallel \boldsymbol{P} \parallel [001]$, and $\boldsymbol{z} \parallel \boldsymbol{M} \parallel [110]$, shown in Fig. 1(d), for convenience of the following formulations.

The net magnetization $\boldsymbol{M}$ and the ferroelectric polarization $\boldsymbol{P}$ are given by sums of the local contributions as $\boldsymbol{M} = \frac{g\mu_B}{NV}\sum_{i=1}^{N}\boldsymbol{m}_i$ and $\boldsymbol{P} = \frac{1}{NV}\sum_{i=1}^{N}\boldsymbol{p}_i$, respectively, where the index i runs over the Cu-ion tetrahedra with *uuud* spins N is the number of tetrahedra, and V ($= 1.76 \times 10^{-28}$ m^3) is the volume per tetrahedron. Because of the cubic symmetry, the local polarization $\boldsymbol{p}_i$ from the ith tetrahedron is given using the spin components m_{ia}, m_{ib}, and m_{ic} in the $P2_13$ setting as

$$\boldsymbol{p}_i = (p_{ia}, p_{ib}, p_{ic}) = \lambda\,(m_{ib}m_{ic}, m_{ic}m_{ia}, m_{ia}m_{ib}). \quad (2)$$

We can easily evaluate the local contributions $\boldsymbol{p}_i$ and $\boldsymbol{m}_i$ from each tetrahedron in the ferrimagnetic phase where all the tetrahedra give uniform contributions. Then the coupling constant λ is evaluated as $\lambda = 5.64 \times 10^{-27}$ μCm from the experimentally measured $P_{[001]} = 16$ μC/m^2 in the ferrimagnetic phase under $\boldsymbol{H} \parallel [111]$ at 5 K.[11]

Because of this strong coupling between magnetism and electricity, collective oscillations of this SkX can be activated not only magnetically by an ac magnetic field $\boldsymbol{H}^\omega$ but also electrically by ac electric field $\boldsymbol{E}^\omega$. As demonstrated below, with the special configuration of $\boldsymbol{P} \perp \boldsymbol{M}$, both the $\boldsymbol{H}^\omega$ and the $\boldsymbol{E}^\omega$ components of an EM wave propagating along $\boldsymbol{P} \times \boldsymbol{M}$ can activate common oscillation modes. To see this, we calculate dynamical magnetic and dielectric susceptibilities,

$$\chi^{\mathrm{mm}}_{\alpha\beta}(\omega) = \frac{M^\omega_\alpha}{\mu_0 H^\omega_\beta}, \quad \chi^{\mathrm{ee}}_{\alpha\beta}(\omega) = \frac{P^\omega_\alpha}{\epsilon_0 E^\omega_\beta}, \quad (3)$$

by numerically solving the Landau-Lifshitz-Gilbert equation using the fourth-order Runge-Kutta method. The equation is given by

$$\frac{d\boldsymbol{m}_i}{dt} = -\boldsymbol{m}_i \times \boldsymbol{H}^{\mathrm{eff}}_i + \frac{\alpha_G}{m}\boldsymbol{m}_i \times \frac{d\boldsymbol{m}_i}{dt}, \quad (4)$$

where α_G ($= 0.04$) is the Gilbert-damping coefficient. The effective field $\boldsymbol{H}^{\mathrm{eff}}_i$ is calculated from the Hamiltonian $\mathcal{H} = \mathcal{H}_0 + \mathcal{H}'(t)$ as $\boldsymbol{H}^{\mathrm{eff}}_i = -\partial\mathcal{H}/\partial\boldsymbol{m}_i$. Here the first term $\mathcal{H}_0$ is the model Hamiltonian, (1), while the perturbation term $\mathcal{H}'(t)$ represents a short rectangular pulse of a magnetic field or electric field. After applying the pulse at $t = 0$, we calculate $\boldsymbol{M}(t)$ and $\boldsymbol{P}(t)$ and obtain their Fourier transforms M^ω_α and P^ω_α. Calculations are performed using a system of $N = 288 \times 288$ sites with the periodic boundary condition.

In Fig. 2(a), we display imaginary parts of the calculated dynamical magnetic susceptibilities, $\mathrm{Im}\chi^{\mathrm{mm}}_{yy}(\omega)$ and $\mathrm{Im}\chi^{\mathrm{mm}}_{zz}(\omega)$, for $\boldsymbol{H}^\omega \parallel \boldsymbol{y}$ and $\boldsymbol{H}^\omega \parallel \boldsymbol{z}$. We also plot the imaginary parts of the calculated dielectric susceptibilities, $\mathrm{Im}\chi^{\mathrm{ee}}_{zz}(\omega)$ and $\mathrm{Im}\chi^{\mathrm{ee}}_{yy}(\omega)$, for $\boldsymbol{E}^\omega \parallel \boldsymbol{z}$ and $\boldsymbol{E}^\omega \parallel \boldsymbol{y}$ in Fig. 2(b). In $\mathrm{Im}\chi^{\mathrm{mm}}_{yy}$, we find a strong resonance active to $\boldsymbol{H}^\omega \parallel \boldsymbol{y}$ at $\omega_R/J = 6.12 \times 10^{-3}$, which was ascribed to the counterclockwise rotation mode, where all the skyrmion cores in the SkX uniformly rotate in the counterclockwise fashion.[32,33] This rotation mode can also be seen in the spectrum of $\mathrm{Im}\chi^{\mathrm{ee}}_{zz}$ as a peak at the same frequency, indicating its simultaneous electric activity to $\boldsymbol{E}^\omega \parallel \boldsymbol{z}$. The spectrum of $\mathrm{Im}\chi^{\mathrm{mm}}_{yy}$ has one more resonance at a higher frequency, $\omega_R = 1.135 \times 10^{-2} J$, which was ascribed to another rotation mode with opposite rotational sense, i.e., the clockwise rotation mode.[32,33] We can see a very tiny peak in $\mathrm{Im}\chi^{\mathrm{ee}}_{zz}$ at the corresponding frequency, indicating its weak

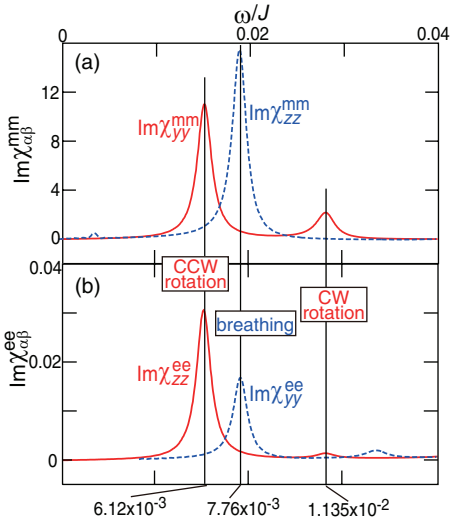

FIG. 2. (Color online) (a) Imaginary parts of the dynamical magnetic susceptibilities, $\mathrm{Im}\chi_{yy}^{\mathrm{mm}}$ and $\mathrm{Im}\chi_{zz}^{\mathrm{mm}}$, as functions of the frequency ω at $g\mu_{\mathrm{B}}\mu_0 H_z/J = 3.75 \times 10^{-3}$. In Ref. 32, the strong (weak) resonance in $\mathrm{Im}\chi_{yy}^{\mathrm{mm}}$ was ascribed to the counterclockwise (clockwise) rotation mode, while the resonance in $\mathrm{Im}\chi_{zz}^{\mathrm{mm}}$ was ascribed to the breathing mode. (b) Imaginary parts of the dynamical dielectric susceptibilities, $\mathrm{Im}\chi_{zz}^{\mathrm{ee}}$ and $\mathrm{Im}\chi_{yy}^{\mathrm{ee}}$, as functions of ω. The three above-mentioned magnetically active resonances can be seen in the spectra of dielectric susceptibilities at the same frequencies, indicating their simultaneous electric activities.

electric activity. On the other hand, the spectrum of $\mathrm{Im}\chi_{zz}^{\mathrm{mm}}$ has a single resonance active to $\boldsymbol{H}^\omega \parallel z$ at $\omega_{\mathrm{R}}/J = 7.76 \times 10^{-3}$, which was ascribed to the breathing mode, where areas of all the skyrmions in the SkX oscillatory expand and shrink in a uniform way.[32,33] Again, this mode is simultaneously active to $\boldsymbol{E}^\omega \parallel \boldsymbol{y}$, and the corresponding peak can be seen in $\mathrm{Im}\chi_{yy}^{\mathrm{ee}}$ at the same frequency. A recent microwave experiment found clear absorptions at these spin-wave resonances, while absorptions at off-resonant frequencies turn out to be negligibly small.[34]

The presence of collective modes active to both $\boldsymbol{E}^\omega$ and $\boldsymbol{H}^\omega$ is nothing but the source of interesting microwave activity. From Maxwell's equations, we can derive the relation $\boldsymbol{H}^\omega \parallel \boldsymbol{K}^\omega \times \boldsymbol{E}^\omega$ for the EM wave. This relation indicates that the relative directions of $\boldsymbol{H}^\omega$ and $\boldsymbol{E}^\omega$ are determined by the propagation vector $\boldsymbol{K}^\omega$, and their relationship should be reversed upon the sign reversal of $\boldsymbol{K}^\omega$. When a lineally polarized EM wave with $\boldsymbol{E}^\omega \parallel z$ and $\boldsymbol{H}^\omega \parallel \boldsymbol{y}$ propagates parallel (antiparallel) to $(\boldsymbol{P} \times \boldsymbol{M}) \parallel \boldsymbol{x}$ as shown in Fig. 3(a), where $\mathrm{sgn}[\mathrm{Re}K^\omega] = +1(\mathrm{sgn}[\mathrm{Re}K^\omega] = -1)$ with $\boldsymbol{K}^\omega = K^\omega \hat{\boldsymbol{x}}$, the oscillation of $\boldsymbol{P}$ induced by $\boldsymbol{E}^\omega$ and that of $\boldsymbol{M}$ by $\boldsymbol{H}^\omega$ contributes in a subtractive (an additive) way to the collective oscillation, which results in weaker (stronger) absorption of the EM wave. Such a nonreciprocal absorption of the EM wave is expected also for $\boldsymbol{E}^\omega \parallel \boldsymbol{y}$ and $\boldsymbol{H}^\omega \parallel z$, as shown in Fig. 3(b).

To study microwave absorption and nonreciprocal directional dichroism (NDD) quantitatively, we start with the following Fourier-formed Maxwell's equations for materials with $\boldsymbol{M}$ and $\boldsymbol{P}$:[35]

$$\omega \boldsymbol{B}^\omega = \boldsymbol{K}^\omega \times \boldsymbol{E}^\omega, \quad -\omega \boldsymbol{D}^\omega = \boldsymbol{K}^\omega \times \boldsymbol{H}^\omega, \tag{5}$$

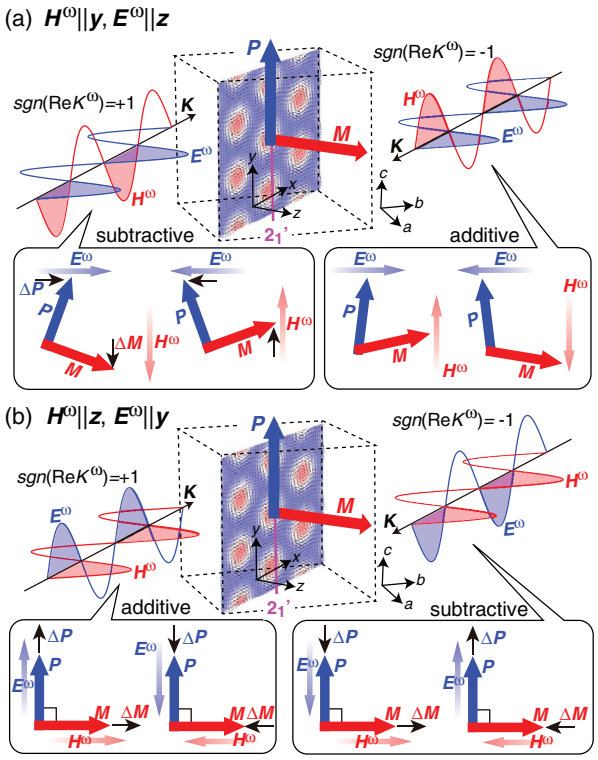

FIG. 3. (Color online) Configurations of the microwave $\boldsymbol{H}^\omega$ and $\boldsymbol{E}^\omega$ components, for which nonreciprocal directional dichroism is expected when $\boldsymbol{P} \parallel \boldsymbol{y}$ and $\boldsymbol{M} \parallel z$ with $\boldsymbol{P} \perp \boldsymbol{M}$ and $\boldsymbol{K}^\omega \parallel \boldsymbol{P} \times \boldsymbol{M} \parallel \boldsymbol{x}$: (a) $\boldsymbol{E}^\omega \parallel z$ and $\boldsymbol{H}^\omega \parallel \boldsymbol{y}$, and (b) $\boldsymbol{E}^\omega \parallel \boldsymbol{y}$ and $\boldsymbol{H}^\omega \parallel z$. Cartesian coordinates $\boldsymbol{x} \parallel [\bar{1}10]$, $\boldsymbol{y} \parallel [001]$, and $\boldsymbol{z} \parallel [110]$ are defined as shown, where the z axis is parallel to $\boldsymbol{H}$.

where

$$\boldsymbol{B}^\omega = \mu_0(\hat{\mu}^\infty \boldsymbol{H}^\omega + \boldsymbol{M}^\omega), \quad \boldsymbol{D}^\omega = \epsilon_0 \hat{\epsilon}^\infty \boldsymbol{E}^\omega + \boldsymbol{P}^\omega, \tag{6}$$

$$\boldsymbol{M}^\omega = \mu_0 \hat{\chi}^{\mathrm{mm}}(\omega)\boldsymbol{H}^\omega + \hat{\chi}^{\mathrm{me}}(\omega)\sqrt{\frac{\epsilon_0}{\mu_0}}\boldsymbol{E}^\omega, \tag{7}$$

$$\boldsymbol{P}^\omega = \epsilon_0 \hat{\chi}^{\mathrm{ee}}(\omega)\boldsymbol{E}^\omega + \hat{\chi}^{\mathrm{em}}(\omega)\sqrt{\epsilon_0\mu_0}\boldsymbol{H}^\omega. \tag{8}$$

As discussed above, NDD of microwaves with $\boldsymbol{K}^\omega = K^\omega \hat{\boldsymbol{x}}$ is expected for the following configurations of $\boldsymbol{H}^\omega$ and $\boldsymbol{E}^\omega$: (i) $\boldsymbol{H}^\omega \parallel \boldsymbol{y}$ and $\boldsymbol{E}^\omega \parallel z$, and (ii) $\boldsymbol{H}^\omega \parallel z$ and $\boldsymbol{E}^\omega \parallel \boldsymbol{y}$. We introduce the complex refractive index $N(\omega) = n(\omega) + i\kappa(\omega)$, which is related to K^ω as $K^\omega = \frac{\omega}{c}N(\omega)$. We solve Eqs. (5) and obtain

$$N(\omega) \sim \sqrt{\left[\epsilon_{zz}^\infty + \chi_{zz}^{\mathrm{ee}}(\omega)\right]\left[\mu_{yy}^\infty + \chi_{yy}^{\mathrm{mm}}(\omega)\right]} - \mathrm{sgn}(\mathrm{Re}K^\omega)\left[\chi_{yz}^{\mathrm{me}}(\omega) + \chi_{zy}^{\mathrm{em}}(\omega)\right]/2 \tag{9}$$

and

$$N(\omega) \sim \sqrt{[\epsilon_{yy}^\infty + \chi_{yy}^{\mathrm{ee}}(\omega)][\mu_{zz}^\infty + \chi_{zz}^{\mathrm{mm}}(\omega)]} + \mathrm{sgn}(\mathrm{Re}K^\omega)[\chi_{zy}^{\mathrm{me}}(\omega) + \chi_{yz}^{\mathrm{em}}(\omega)]/2 \tag{10}$$

for cases (i) and (ii), respectively. These expressions contain the sign of $\mathrm{Re}K^\omega$ indicating the direction dependence of the microwave absorption because the absorption coefficient $\alpha(\omega)$

is related to $N(\omega)$ as

$$\alpha(\omega) = \frac{2\omega\kappa(\omega)}{c} \propto \omega \mathrm{Im}N(\omega),$$

and the absorption intensity is given by $I(\omega) = I_0 \exp[-\alpha(\omega)l]$, where l is the sample thickness. The nonreciprocal absorption $\Delta\alpha(\omega) = \alpha_+(\omega) - \alpha_-(\omega)$ represents the magnitude of NDD, where α_+ and α_- are absorption coefficients for microwaves propagating in the positive and negative directions, respectively.

In order to evaluate $N(\omega)$ and $\alpha_\pm(\omega)$ quantitatively, we need to calculate not only the dielectric and magnetic susceptibilities but also the following dynamical ME susceptibilities:

$$\chi^{\mathrm{em}}_{\alpha\beta}(\omega) = \frac{P^\omega_\alpha}{\sqrt{\epsilon_0\mu_0}H^\omega_\beta}, \quad \chi^{\mathrm{me}}_{\alpha\beta}(\omega) = \sqrt{\frac{\mu_0}{\epsilon_0}}\frac{M^\omega_\alpha}{E^\omega_\beta}. \qquad (11)$$

For the values of ϵ^∞_{zz} and ϵ^∞_{yy} in Eqs. (9) and (10), we assume an isotropic dielectric tensor, i.e., $\epsilon^\infty_{zz} = \epsilon^\infty_{yy} = \epsilon^\infty$, for simplicity and set $\epsilon^\infty = 8$ according to the dielectric-measurement data.[22,36] In turn, we take $\mu^\infty_{zz} = \mu^\infty_{yy} = 1$ for permeability. The value of J is set to be $J = 1$ meV so as to reproduce the experimental T_c for the SkX-paramagnetic transition.

In Figs. 4(a) and 4(b), we display the calculated ω dependence of the absorption coefficients, $\alpha_+(\omega)$ and $\alpha_-(\omega)$, at several values of H_z for $\boldsymbol{E}^\omega \parallel z$ and $\boldsymbol{H}^\omega \parallel \boldsymbol{y}$ for $\boldsymbol{E}^\omega \parallel \boldsymbol{y}$ and $\boldsymbol{H}^\omega \parallel z$, respectively. The out-of-plane $\boldsymbol{E}^\omega \parallel z$ and in-plane $\boldsymbol{H}^\omega \parallel \boldsymbol{y}$ activate two rotation modes with opposite senses,[32,33] i.e., lower-lying counterclockwise and higher-lying clockwise modes, which give two spectral peaks in Fig. 4(a). We find that, for the lower-lying resonance, the $\Delta\alpha(\omega)$ increases as H_z increases and reaches more than 0.25 cm^{-1}, which corresponds to a relative change $\Delta\alpha/\alpha_{\mathrm{ave}} = 2(\alpha_+ - \alpha_-)/(\alpha_+ + \alpha_-) \sim 20\%$ at maximum. On the other hand, both the in-plane $\boldsymbol{E}^\omega \parallel \boldsymbol{y}$ and the out-of-plane $\boldsymbol{H}^\omega \parallel z$ activate a breathing mode,[32,33] which gives a single spectral peak in Fig. 4(b). Again, the $\Delta\alpha(\omega)$ increases with increasing H_z and reaches approximately 0.14 cm^{-1}, corresponding to a $\Delta\alpha/\alpha_{\mathrm{ave}}$ of 10%. These values do not depend on the value of α_{G}. Such a huge directional dichroism is quite rare for any frequency range[35,37–39] and has never been realized at gigahertz frequencies. This is because most of the multiferroics with simple magnetic orders have resonant frequencies much higher than microwave frequencies due to the large spin gaps. In turn, the long-period skyrmion textures have small spin gaps and their nontrivial collective modes with gigahertz frequencies enable us to achieve interesting microwave functions.

In summary, we have theoretically predicted that the SkX phase of the chiral-lattice insulator Cu_2OSeO_3 shows an enhanced diode effect on linearly polarized microwaves as a consequence of interference between magnetic and electric responses from the multiferroic skyrmion texture. Our prediction demonstrates that the skyrmion and the SkX host interesting dynamical phenomena in the microwave frequency regimes in addition to the peculiar transport and spintronics phenomena.

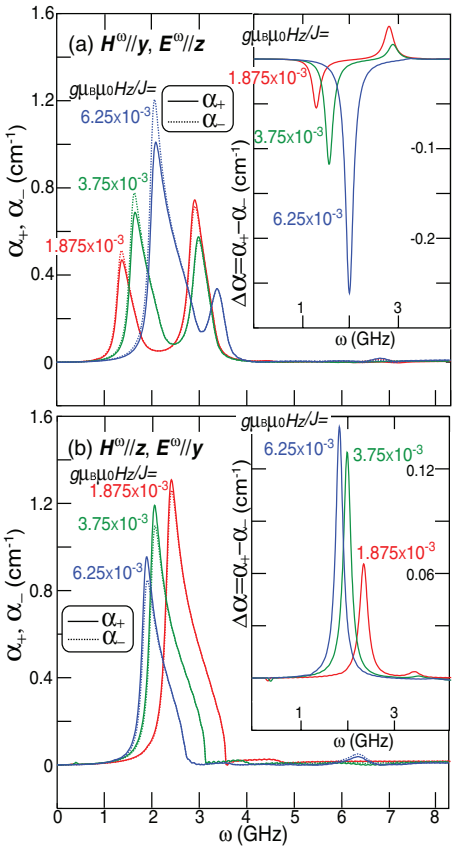

FIG. 4. (Color online) Calculated absorption coefficients, $\alpha_+(\omega)$ and $\alpha_-(\omega)$, for microwaves with $\mathrm{sgn}(\mathrm{Re}K^\omega) = +1$ and $\mathrm{sgn}(\mathrm{Re}K^\omega) = -1$, respectively, at several values of H_z in the cases of (a) $\boldsymbol{H}^\omega \parallel \boldsymbol{y}$ and $\boldsymbol{E}^\omega \parallel z$ and (b) $\boldsymbol{H}^\omega \parallel z$ and $\boldsymbol{E}^\omega \parallel \boldsymbol{y}$.

The authors thank A. Rosch, N. Nagaosa, Y. Tokura, and N. Furukawa for discussions. M.M. thanks the University of Cologne for hospitality. This work was supported by the Japan Society for the Promotion of Science (JSPS) through the "Funding Program for World-Leading Innovative R&D on Science and Technology" (FIRST Program), by the G-COE Program "Physical Sciences Frontier" from MEXT Japan, by the PRESTO Program of the JST, and by the Murata Science Foundation.

*Corresponding author: mochizuki@ap.t.u-tokyo.ac.jp

[1] T. H. R. Skyrme, Nucl. Phys. **31**, 556 (1962).
[2] A. N. Bogdanov and D. A. Yablonskii, Sov. Phys. JETP **68**, 101 (1989).
[3] U. K. Rößler, A. N. Bogdanov, and C. Pfleiderer, Nature **442**, 797 (2006).
[4] S. Mühlbauer, B. Binz, F. Jonietz, C. Pfleiderer, A. Rosch, A. Neubauer, R. Georgii, and P. Böni, Science **323**, 915 (2009).
[5] C. Pappas, E. Lelievère-Berna, P. Falus, P. M. Bentley, E. Moskvin, S. Grigoriev, P. Fouquet, and B. Farago, Phys. Rev. Lett. **102**, 197202 (2009).
[6] C. Pfleiderer, T. Adams, A. Bauer, W. Biberacher, B. Binz, F. Birkelbach, P. Böni, C. Franz, R. Georgii, M. Janoschek, F. Jonietz, T. Keller, R. Ritz, S. Mühlbauer, W. Munzer, A. Neubauer, B. Pedersen, and A. Rosch, J. Phys.: Condens. Matter **22**, 164207 (2010).

[7]T. Adams, S. Mühlbauer, C. Pfleiderer, F. Jonietz, A. Bauer, A. Neubauer, R. Georgii, P. Böni, U. Keiderling, K. Everschor, M. Garst, and A. Rosch, Phys. Rev. Lett. **107**, 217206 (2011).
[8]W. Munzer, A. Neubauer, T. Adams, S. Mühlbauer, C. Franz, F. Jonietz, R. Georgii, P. Böni, B. Pedersen, M. Schmidt, A. Rosch, and C. Pfleiderer, Phys. Rev. B **81**, 041203(R) (2010).
[9]X. Z. Yu, Y. Onose, N. Kanazawa, J. H. Park, J. H. Han, Y. Matsui, N. Nagaosa, and Y. Tokura, Nature (London) **465**, 901 (2010).
[10]X. Z. Yu, N. Kanazawa, Y. Onose, K. Kimoto, W. Z. Zhang, S. Ishiwata, Y. Matsui, and Y. Tokura, Nat. Mater. **10**, 106 (2010).
[11]S. Seki, X. Z. Yu, S. Ishiwata, and Y. Tokura, Science **336**, 198 (2012).
[12]T. Adams, A. Chacon, M. Wagner, A. Bauer, G. Brandl, B. Pedersen, H. Berger, P. Lemmens, and C. Pfleiderer, Phys. Rev. Lett. **108**, 237204 (2012).
[13]S. Seki, J.-H. Kim, D. S. Inosov, R. Georgii, B. Keimer, S. Ishiwata, and Y. Tokura, Phys. Rev. B **85**, 220406 (2012).
[14]B. Binz and A. Vishwanath, Physica B **403**, 1336 (2008).
[15]A. Neubauer, C. Pfleiderer, B. Binz, A. Rosch, R. Ritz, P. G. Niklowitz, and P. Böni, Phys. Rev. Lett. **102**, 186602 (2009).
[16]N. Kanazawa, Y. Onose, T. Arima, D. Okuyama, K. Ohoyama, S. Wakimoto, K. Kakurai, S. Ishiwata, and Y. Tokura, Phys. Rev. Lett. **106**, 156603 (2011).
[17]C. Pfleiderer and A. Rosch, Nature **465**, 880 (2010).
[18]T. Schulz, R. Ritz, A. Bauer, M. Halder, M. Wagner, C. Franz, C. Pfleiderer, K. Everschor, M. Garst, and A. Rosch, Nat. Phys. **8**, 301 (2012).
[19]S. X. Huang and C. L. Chien, Phys. Rev. Lett. **108**, 267201 (2012).
[20]F. Jonietz, S. Mühlbauer, C. Pfleiderer, A. Neubauer, W. Munzer, A. Bauer, T. Adams, R. Georgii, P. Böni, R. A. Duine, K. Everschor, M. Garst, and A. Rosch, Science **330**, 1648 (2010).
[21]X. Z. Yu, N. Kanazawa, W. Z. Zhang, T. Nagai, T. Hara, K. Kimoto, Y. Matsui, Y. Onose, and Y. Tokura, Nature Commun. **3**, 988 (2012).
[22]M. Belesi, I. Rousochatzakis, M. Abid, U. K. Rößler, H. Berger, and J.-Ph. Ansermet, Phys. Rev. B **85**, 224413 (2012).
[23]S. Seki, S. Ishiwata, and Y. Tokura, Phys. Rev. B **86**, 060403 (2012).
[24]J. S. White, I. Levatić, A. A. Omrani, N. Egetenmeyer, K. Prša, I. Živković, J. L. Gavilano, J. Kohlbrecher, M. Bartkowiak, H. Berger, and H. M. Rønnow, J. Phys.: Condens. Matter **24**, 432201 (2012).
[25]A. G. Gurevich and G. A. Melkov, *Magnetization Oscillation and Waves* (CRC Pess, New York, 1996).
[26]J.-W. G. Bos, C. V. Colin, and T. T. M. Palstra, Phys. Rev. B **78**, 094416 (2008).
[27]M. Belesi, I. Rousochatzakis, H. C. Wu, H. Berger, I. V. Shvets, F. Mila, and J. P. Ansermet, Phys. Rev. B **82**, 094422 (2010).
[28]P. Bak and M. H. Jensen, J. Phys. C **13**, L881 (1980).
[29]S. D. Yi, S. Onoda, N. Nagaosa, and J. H. Han, Phys. Rev. B **80**, 054416 (2009).
[30]J. H. Han, J. Zang, Z. Yang, J.-H. Park, and N. Nagaosa, Phys. Rev. B **82**, 094429 (2010).
[31]J. H. Yang, Z. L. Li, X. Z. Lu, M.-H. Whangbo, S.-Hi. Wei, X. G. Gong, and H. J. Xiang, Phys. Rev. Lett. **109**, 107203 (2012).
[32]M. Mochizuki, Phys. Rev. Lett. **108**, 017601 (2012).
[33]O. Petrova and O. Tchernyshyov, Phys. Rev. B **84**, 214433 (2011).
[34]Y. Onose, Y. Okamura, S. Seki, S. Ishiwata, and Y. Tokura, Phys. Rev. Lett. **109**, 037603 (2012).
[35]I. Kézsmárki, N. Kida, H. Murakawa, S. Bordács, Y. Onose, and Y. Tokura, Phys. Rev. Lett. **106**, 057403 (2011).
[36]K. H. Miller, X. S. Xu., H. Berger, E. S. Knowles, D. J. Arenas, M. W. Meisel, and D. B. Tanner, Phys. Rev. B **82**, 144107 (2010).
[37]Y. Takahashi, R. Shimano, Y. Kaneko, H. Murakawa, and Y. Tokura, Nat. Phys. **8**, 121 (2012).
[38]S. Bordács, I. Kézsmárki, D. Szaller, L. Demko, N. Kida, H. Murakawa, Y. Onose, R. Shimano, T. Rõõm, U. Nagel, S. Miyahara, N. Furukawa, and Y. Tokura, Nat. Phys. **8**, 734 (2012).
[39]S. Miyahara and N. Furukawa, J. Phys. Soc. Jpn. **80**, 073708 (2011).